

## $\gamma$ Rays Following Thermal Neutron Capture in Titanium

J. W. KNOWLES, G. MANNING\*, G. A. BARTHOLOMEW, AND P. J. CAMPION  
*General Physics Branch, Atomic Energy of Canada Limited, Chalk River, Ontario, Canada*  
 (Received December 18, 1958)

The  $\gamma$  rays following thermal neutron capture in titanium have been studied with two high resolution spectrometers and with an angular correlation arrangement using two sodium iodide scintillation spectrometers. The high resolution instruments were a pair spectrometer for the energy range 2.8 to 11.0 Mev and a double flat crystal diffraction spectrometer for the energy range 0.14 to 5 Mev. A total of 54  $\gamma$  rays were observed, 25 of which had not previously been resolved. A decay scheme for  $Ti^{49}$  is given with energy levels at  $1.378 \pm 0.001$ ,  $1.583 \pm 0.001$ ,  $1.719 \pm 0.001$ ,  $3.172 \pm 0.002$ , and  $3.261 \pm 0.005$  Mev. The neutron binding energy of  $Ti^{49}$  is concluded to be  $8.132 \pm 0.006$  Mev. Angular correlation measurements were made between some of the prominent  $\gamma$  rays emitted in the decay of  $Ti^{49}$ . The measurements confirm that the spins of the 1.378 and 1.719 Mev levels are  $\frac{3}{2}$  and  $\frac{1}{2}$ , respectively.

### I. INTRODUCTION

THE  $\gamma$  rays following thermal neutron capture in natural titanium have been the subject of many previous investigations. The spectrum has been studied with high resolution spectrometers by Kinsey and Bartholomew,<sup>1</sup> Motz,<sup>2</sup> and by Adyasevich, Groshev, and Demidov.<sup>3</sup> Other authors, Hamermesh and Hummel,<sup>4</sup> Braid,<sup>5</sup> Reier and Shamos,<sup>6</sup> and Segel,<sup>7</sup> have used various forms of sodium iodide scintillation spectrometers. In addition, Trumpy<sup>8</sup> has measured the circular polarization of  $\gamma$  radiation following capture of polarized thermal neutrons in titanium. The present paper reports measurements made at the Chalk River Laboratories with two high-resolution spectrometers and with an angular correlation apparatus using two sodium iodide crystals in coincidence. The resolution of the present measurements, one percent or better over most of the energy range, represents a considerable improvement over that of earlier work and has led to the detection of some 25 previously unreported  $\gamma$  rays. This, together with the high accuracy of the energy measurements (better than 0.1% for many of the lines), has provided useful information on the decay schemes of the titanium isotopes. The angular correlation apparatus was used to study three  $\gamma$ -ray cascades in  $Ti^{49}$  and the results confirm that the spins of the 1.378- and 1.719-Mev levels are  $\frac{3}{2}$  and  $\frac{1}{2}$ , respectively.<sup>8</sup>

### II. APPARATUS

The high resolution measurements were made using a collimated beam of  $\gamma$  rays from a 3.5 kg target of

titanium metal<sup>9</sup> placed in the NRX reactor. The two instruments used were a pair spectrometer<sup>10</sup> and a flat crystal diffraction spectrometer.<sup>11</sup> These were arranged at the same experimental hole of the reactor, the  $\gamma$  rays being transmitted through the pair spectrometer to the crystal spectrometer.

#### IIA. Pair Spectrometer

The pair spectrometer has previously been described<sup>10</sup> and earlier measurements with it on the neutron capture spectrum from titanium have been reported in a previous paper.<sup>1</sup> The results presented here were obtained using the same spectrometer with a modified slit system in front of the stilbene crystals.<sup>12</sup> The modified slits made the spectrometer line approximately a constant fraction of the energy and also improved the line shape by largely eliminating the low-energy tail. The majority of the measurements, Fig. 1., were made with a resolution of one percent. Some regions of interest were studied with a slightly better resolution, *viz.*, 0.8%. The earlier results<sup>1</sup> were obtained with a constant line width of about 100 kev and hence the later measurements represent a substantial improvement in resolution especially at the lower energies. The region from 9.5 to 11.0 Mev, which contains  $\gamma$  rays of low intensity, was studied under conditions of higher efficiency but poorer resolution (line width of 180 kev).

#### IIB. Flat Crystal Diffraction Spectrometer

The low-energy region of the spectrum was investigated using the flat crystal diffraction spectrometer. Details of its design and operation are given elsewhere

\* Now at Norman Bridge Laboratory of Physics, California Institute of Technology, Pasadena, California.

<sup>1</sup> B. B. Kinsey and G. A. Bartholomew, *Phys. Rev.* **89**, 375 (1953).

<sup>2</sup> H. T. Motz, *Phys. Rev.* **93**, 925 (1954).

<sup>3</sup> Adyasevich, Groshev, and Demidov, *Atomnaya Energ.* **1**, 40 (1956).

<sup>4</sup> B. Hamermesh and V. Hummel, *Phys. Rev.* **88**, 916 (1952).

<sup>5</sup> T. H. Braid, *Phys. Rev.* **102**, 1109 (1956).

<sup>6</sup> M. Reier and M. H. Shamos, *Phys. Rev.* **100**, 1302 (1955).

<sup>7</sup> R. E. Segel, *Bull. Am. Phys. Soc. Ser. II*, **2**, 230 (1957).

<sup>8</sup> G. Trumpy, *Nuclear Phys.* **2**, 664 (1956).

<sup>9</sup> Spectroscopic analysis of the target material showed that the most abundant impurities, Na, Al, Fe, and W, were present in concentrations too low to produce detectable  $\gamma$  rays anywhere in the spectrum except near 7.7 Mev, see Table I.

<sup>10</sup> B. B. Kinsey and G. A. Bartholomew, *Can. J. Phys.* **31**, 537 (1953).

<sup>11</sup> J. W. Knowles, *Can. J. Phys.* **37**, 203, (1959) See also *Bull. Am. Phys. Soc. Ser. II*, **2**, 16 (1957); and Chalk River Report GPI-42, 1957 (unpublished).

<sup>12</sup> Bartholomew, Campion, and Robinson (to be published).

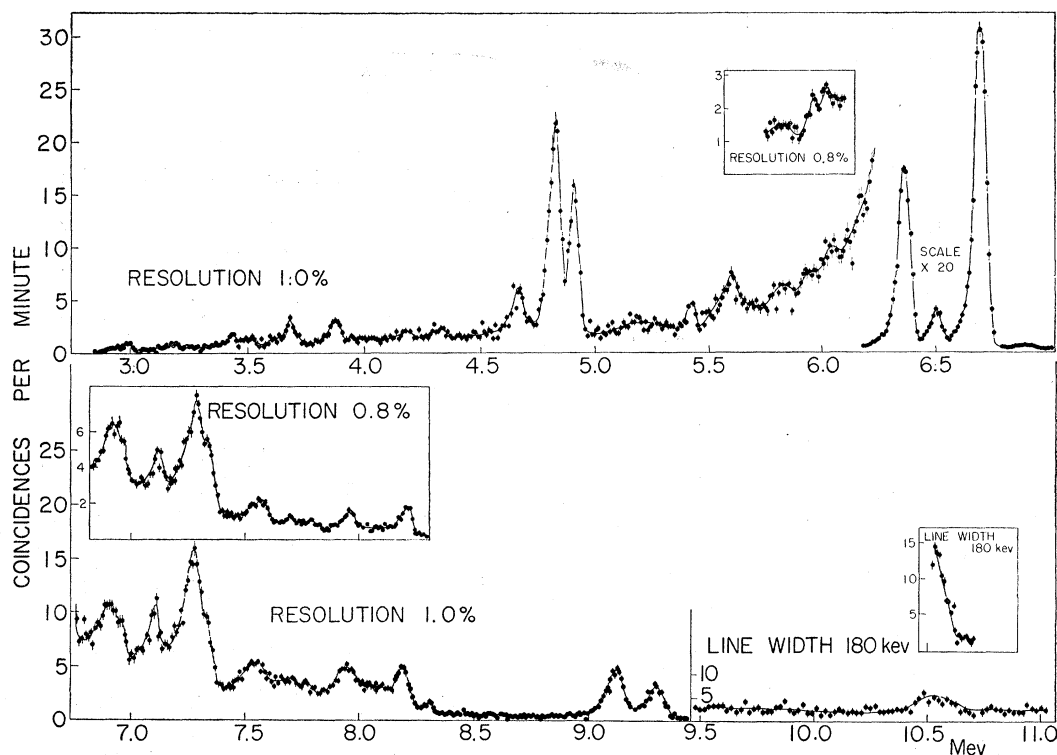


Fig. 1. Gamma-ray spectrum from 2.8 to 11 Mev. The curves show the pair spectrometer counting rate uncorrected for spectrometer efficiency and absorption of the  $\gamma$  rays.

by Knowles.<sup>11</sup> For the measurements shown in Fig. 2., three spectrometer arrangements were used. The  $\gamma$  rays in the region *A*, 0.50 to 1.9 Mev, were Laue diffracted from the (211) planes of two 23-mm thick calcite crystals set in the antiparallel position. For the region *A'*, 1.80 to 5.1 Mev, it was more efficient to use two calcite crystals, each 62 mm thick. The thicker crystals did not give the best efficiency below 1.8 Mev because in this energy range they strongly absorb the diffracted beam and, in addition, broaden<sup>11</sup> the lines, thereby reducing the energy resolution. Because two sets of diffracting crystals of different thickness were used and because the diffraction line width decreases with the diffraction angle, the measured spectrum has nearly constant resolution, 0.4 to 0.6%, from 0.34 to 5 Mev. In region *B*, 0.14 to 0.52 Mev, a single crystal arrangement consisting of a single calcite crystal and a system of Soller slits was used. The resolution for this arrangement, determined by the 45 second angular divergence of the slit system, was 2.2% in the region of 0.2 Mev.

### IIC. Angular Correlation Apparatus

Angular correlation measurements were made on three of the strongest cascades emitted in the decay of the product nucleus  $Ti^{40}$ . Full details of the apparatus used are given by Manning and Bartholomew.<sup>13</sup> The

<sup>13</sup> G. Manning and G. A. Bartholomew (to be published).

measurements were made using a collimated thermal neutron beam which bombarded a target of titanium metal 0.5 inch in diameter and one inch long. The NaI (Tl) crystals used were 4 inches in diameter and 6 inches long and were mounted on 5-inch DuMont 6364 photomultiplier tubes. The two counters were well shielded from general background radiation by a lead box with five-inch-thick walls surrounded by a ten-inch-thick neutron shield of paraffin wax and boracic acid. A  $Li^6$  metal shield was placed between the target and the counters to absorb neutrons scattered from the target. The coincidence electronics used was a conventional fast-slow arrangement with a resolving time,  $\tau$ , of about  $2 \times 10^{-8}$  second. The spectrum from one counter in coincidence with a narrow pulse-height range in the other counter was recorded in a 100-channel pulse-height analyzer.<sup>14</sup> The angle between the NaI detectors could be varied between  $90^\circ$  and  $220^\circ$  permitting the measurement of angular correlation between coincident  $\gamma$ -rays.

## III. EXPERIMENTAL DETAILS AND RESULTS

### IIIA. Pair Spectrometer

The region from 2.8 to 11.0 Mev was examined with the pair spectrometer and a total of 34  $\gamma$  rays were resolved. The spectrum obtained, uncorrected for

<sup>14</sup> F. S. Goulding, Nat. Acad. Sci. Nat. Research Council Publ. No. 467, 86 (1957).

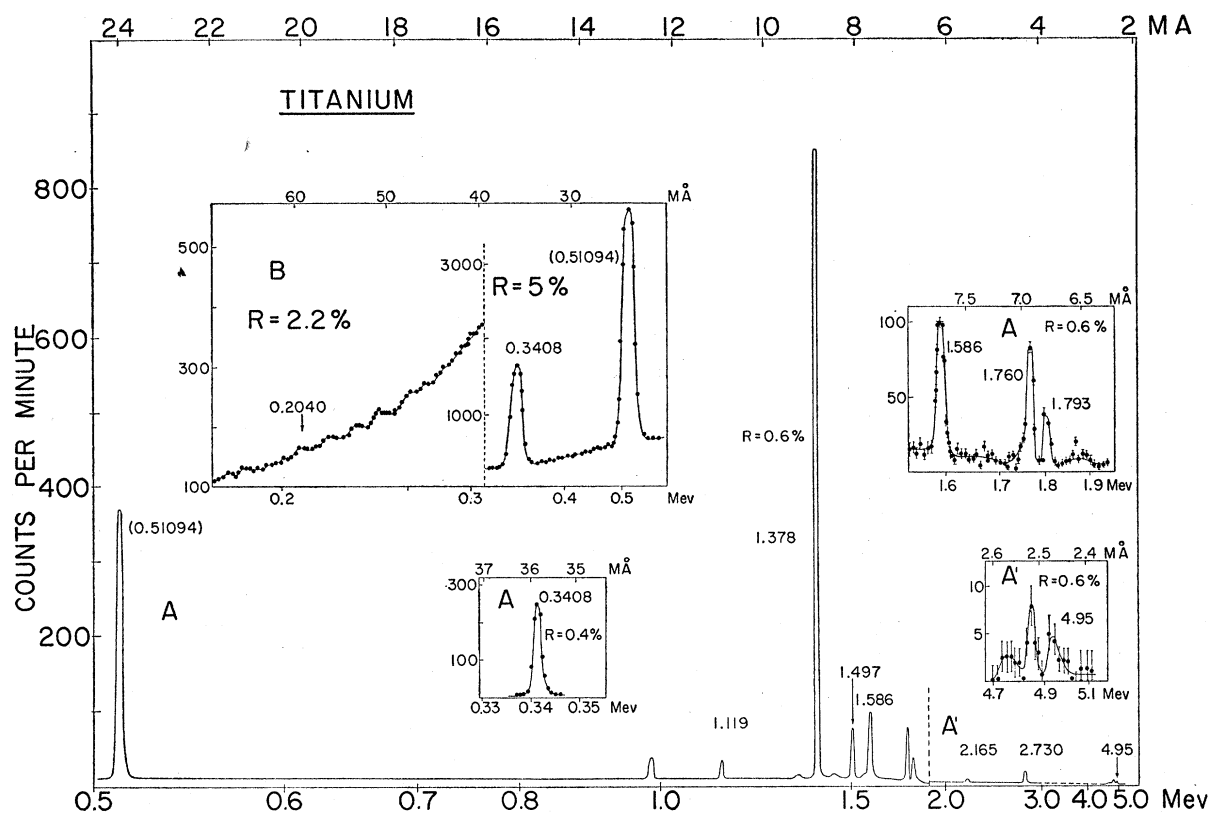


FIG. 2. Gamma-ray spectrum from 0.14 to 5 Mev plotted on a linear MA scale. The undiffracted background has been subtracted from the measurements but no corrections have been applied for spectrometer efficiency and source absorption. For the double crystal measurements, in region A, 0.5 to 1.9 Mev, two calcite crystals 23 mm thick were used and in region A', 1.80 to 5 Mev, the crystals were 62 mm thick. In the region B, 0.14 to 0.52 Mev, a single crystal arrangement was used which consisted of a system of Soller slits and a single calcite crystal. In all arrangements, the radiation was Laue diffracted from the (211) planes of the crystals. All  $\gamma$ -ray energies are measured relative to that of the annihilation radiation, 0.51094 Mev.<sup>17</sup>

spectrometer efficiency and  $\gamma$ -ray absorption, is shown in Fig. 1. Table I contains a list of the observed  $\gamma$  rays and their absolute intensities together with the results of Adyasevich *et al.*<sup>3</sup> The absolute intensities were determined by comparing the counting rates of the titanium  $\gamma$  rays with the counting rate for the 9.0-Mev  $\gamma$  ray of nickel from a known mixture of titanium and nickel oxides. Details of this method<sup>15</sup> have been published by Kinsey *et al.*<sup>10,16</sup> The estimated accuracy of the quoted intensities for strong well-resolved lines is nowhere better than  $\pm 20\%$  and may be considerably worse for some of the weaker lines. The agreement between the pair spectrometer determinations of energy and intensity and those of Adyasevich *et al.* is satisfactory.

<sup>15</sup> The thermal neutron capture cross sections of titanium,  $5.8 \pm 0.4$  barns, and sodium,  $0.536 \pm 0.010$  barn, which enter this determination were taken from the tables of *Neutron Cross Sections*, compiled by D. J. Hughes and R. Schwartz, Brookhaven National Laboratory Report BNL-325, Suppl. No. 1 (Superintendent of Documents, U. S. Government Printing Office, Washington, D. C., 1958), second edition.

<sup>16</sup> Kinsey, Bartholomew, and Walker, *Phys. Rev.* **83**, 519 (1951).

### IIIB. Diffraction Spectrometer

The diffraction spectrometer was used to study the region from 0.14 to 5 Mev. The observed spectrum is shown in Fig. 2. Table II contains a list of the resolved  $\gamma$  rays together with the results of Motz<sup>2</sup> and of Adyasevich *et al.*<sup>3</sup> which are shown for comparison. All  $\gamma$ -ray energies were measured relative to that of the annihilation  $\gamma$  ray, 0.51094 Mev.<sup>17</sup> The absolute intensities of the  $\gamma$  rays measured by the diffraction spectrometer were determined by a comparison method using a mixture of  $V_2O_5$  and  $TiO_2$  of accurately known proportions. The intensity of the 1.378-Mev neutron capture  $\gamma$  ray from titanium was compared with that of the 1.45-Mev  $\gamma$  ray associated with the  $\beta$  decay of  $V^{52}$  at equilibrium. In a previous comparison with sodium<sup>18</sup> it has been shown that the product of the cross section of natural vanadium and the number of 1.45-Mev photons per neutron captured at equilibrium is equal to  $4.73 \pm 0.15$  barn photons per capture in natural vanadium. Using this value the corresponding

<sup>17</sup> Muller, Hoyt, Klein, and DuMond, *Phys. Rev.* **88**, 775 (1952).

<sup>18</sup> J. W. Knowles (to be published).

TABLE I. Energies and intensities of titanium  $\gamma$  rays above 3.0 Mev.

Pair spectrometer		Compton spectrometer <sup>a</sup>		Diffraction spectrometer	
Energy in Mev	Intensity <sup>b</sup>	Energy in Mev	Intensity <sup>b</sup>	Energy in Mev	Intensity <sup>b</sup>
10.621±0.014	0.03	10.47 ±0.15	0.01		
9.376±0.012	0.08	9.39 ±0.05	0.09		
9.189±0.011	0.08	9.17 ±0.07	0.13		
8.342±0.011	0.05				
8.252±0.010	0.17	8.31 ±0.05	0.2		
7.996±0.012	0.08				
7.844±0.015	0.03				
(7.736±0.013)	(0.03) <sup>c</sup>				
(7.628±0.011)	(0.08) <sup>c</sup>	7.66 ±0.04	0.3		
7.55 ±0.02	0.04				
7.386±0.009	0.3				
7.319±0.010	0.4				
7.149±0.010	0.3	7.16 ±0.05	0.6		
6.996±0.010	0.3				
6.947±0.014	0.17				
6.753±0.005	41	6.756±0.01	38		
6.550±0.008	5.9	6.56 ±0.03	4		
6.413±0.005	29	6.42 ±0.02	27.5		
6.07 ±0.02	0.17				
5.98 ±0.02	0.08				
5.89 ±0.02	0.17				
5.644±0.012	0.5	5.67 ±0.06	0.8		
5.460±0.014	0.4				
4.957±0.006	3.4	4.96 ±0.02	2.7	4.95±0.02	3.0
4.871±0.006	5.0	4.875±0.02	5.2	4.85±0.02	5.6
4.706±0.013	1.3	4.68 ±0.03	2	4.75±0.03	2.0
4.38 ±0.02	0.3	(4.3 ±0.06)	0.6		
4.22 ±0.02	0.3				
3.916±0.010	1.4	3.86 ±0.02	2.1		
3.733±0.014	1.8	3.65 ±0.02	2.4		
3.55 ±0.02	0.7	3.5 ±0.03	1.2		
3.460±0.015	1.1	3.39 ±0.03	2.6		
3.23 ±0.02	0.7	3.20 ±0.04	1.3		
3.028±0.014	1.8	3.02 ±0.04	2.8		

<sup>a</sup> See reference 3.

<sup>b</sup> Intensity in photons per 100 captures in natural titanium.

<sup>c</sup> These peaks may be produced in part by radiation from iron and aluminum.

product for the 1.378-Mev neutron capture  $\gamma$  ray in titanium was found to be  $4.73 \pm 0.25$  barn photons per capture; so that the absolute intensity of the 1.378 Mev  $\gamma$  ray is  $0.82 \pm 0.08$  photons per capture<sup>15</sup> in natural titanium. The absolute intensities of the other  $\gamma$  rays listed in Table II were calculated from that of the 1.378-Mev  $\gamma$  ray.<sup>19</sup> The accuracy of the relative intensities is approximately  $\pm 15\%$  for strong well-resolved lines but may be considerably worse for some of the weaker lines. A rough measurement was made of the  $\gamma$  rays in the region of 4.9 Mev, see inset in Fig. 2. A measurement of the intensity of these  $\gamma$  rays, see Table I, agrees favorably with those made with the Compton spectrometer,<sup>3</sup> and with the present pair spectrometer.

The greater resolution of the diffraction spectrometer enabled the line reported by Motz<sup>2</sup> and by Adyasevich *et al.*<sup>3</sup> at 1.78 Mev to be resolved into two lines at 1.793 and 1.760 Mev. Measurement of the shape of the 1.586-Mev line, Fig. 3, showed it to be broader than a

<sup>19</sup> If it is assumed<sup>15</sup> that 95% of the total cross section of titanium is due to  $Ti^{49}$ , the absolute intensity of the 1.378-Mev  $\gamma$  ray is calculated to be  $0.86 \pm 0.08$  photon per capture in  $Ti^{49}$ . This is in agreement with the decay scheme for  $Ti^{49}$ , Fig. 8, which attributes at least 13% of the transitions to the ground state to  $\gamma$  rays other than the 1.378-Mev transition.

single  $\gamma$ -ray line at that energy. The single  $\gamma$ -ray line shape was measured at a mean energy of 1.586 Mev by using the spectrometer in its parallel position. A check that the parallel and antiparallel arrangements<sup>11</sup> gave the same line shape for a single  $\gamma$  ray was made on the neighboring 1.378-Mev  $\gamma$  ray. If it is assumed that the 1.586-Mev line is produced by two  $\gamma$  rays, the data is best fitted by  $\gamma$  rays of approximately equal intensity at 1.583 and 1.589 Mev. There is some disagreement between our results and those of Adyasevich *et al.*<sup>3</sup> near 1 Mev and between 2 and 3 Mev, see Table II. A careful search of these regions failed to show some lines of energy and intensity quoted by these workers.

### IIIC. Angular Correlation Results

Coincidence measurements between cascade  $\gamma$  rays following thermal neutron capture in titanium have been made by Segel.<sup>7</sup> The measurements reported here confirm that the following pairs of  $\gamma$  rays are in coincidence: 6.75–1.38; 6.41–1.38; 6.41–0.34; and 1.38–0.34 Mev (the 6.75 and 6.41  $\gamma$  rays could not be resolved but the relative proportion of them accepted by a differential discriminator could be changed by varying the position of the discriminators). The position of these cascade pairs in the decay scheme of  $Ti^{49}$  is shown in Fig. 8.

TABLE II. Energies and intensities of titanium  $\gamma$  rays below 3.0 Mev.

Diffraction spectrometer		Compton spectrometer <sup>a</sup>		Lens spectrometer <sup>b</sup>	
Energy in Mev	Intensity <sup>c</sup>	Energy in Mev	Intensity <sup>c</sup>	Energy in Mev	Relative intensity
2.730 $\pm 0.002$	1.4	2.95 $\pm 0.04$	1.5		
2.165 $\pm 0.002$	0.6	2.83 $\pm 0.04$	1.5		
		2.22 $\pm 0.03$	2.85		
		2.08 $\pm 0.03$	2.4		
1.793 $\pm 0.001$	1.6	1.78 $\pm 0.02$	7.5	1.785	7
1.760 $\pm 0.001$	4.4				
1.589 $\pm 0.001$	4.4	1.60 $\pm 0.01$	13.0	1.590	13
1.583 $\pm 0.001$	4.4				
1.497 $\pm 0.001$	3.8	1.51 $\pm 0.01$	5.2	1.500	5
1.438 $\pm 0.002$	1.3				
1.378 $\pm 0.001$	82	1.39 $\pm 0.005$	85	1.385	90
1.320 $\pm 0.003$	0.5				
1.119 $\pm 0.002$	1.4	1.18 $\pm 0.02$	2.8		
0.984 $\pm 0.002$	1.5	1.03 $\pm 0.02$	5.7		
0.3408 $\pm 0.0003$	29	0.35 $\pm 0.005$	24	0.346	
0.2530 $\pm 0.0005$	0.4				
0.2348 $\pm 0.0005$	0.8				
0.2260 $\pm 0.0005$	0.4				
0.2160 $\pm 0.0005$	0.5				
0.2040 $\pm 0.0005$	0.7				
0.1860 $\pm 0.0005$	0.8				
0.1805 $\pm 0.0005$	0.8				

<sup>a</sup> See reference 3.  
<sup>b</sup> See reference 2.  
<sup>c</sup> Intensity in photons per 100 captures in natural titanium.

Proton angular distributions from the  $Ti^{48}(d,p)Ti^{49}$  reaction studied by Bretscher *et al.*<sup>20</sup> indicated that the levels at 1.378 and 1.719 Mev have spins of  $\frac{1}{2}^-$  or  $\frac{3}{2}^-$  and negative parity. Trumpy<sup>8</sup> measured the circular

polarizations of the 6.75 and 6.41 Mev  $\gamma$  rays following capture of polarized thermal neutrons and concluded that the 1.378- and 1.719-Mev levels are  $\frac{3}{2}^-$  and  $\frac{1}{2}^-$ , respectively. In the experiments reported here three

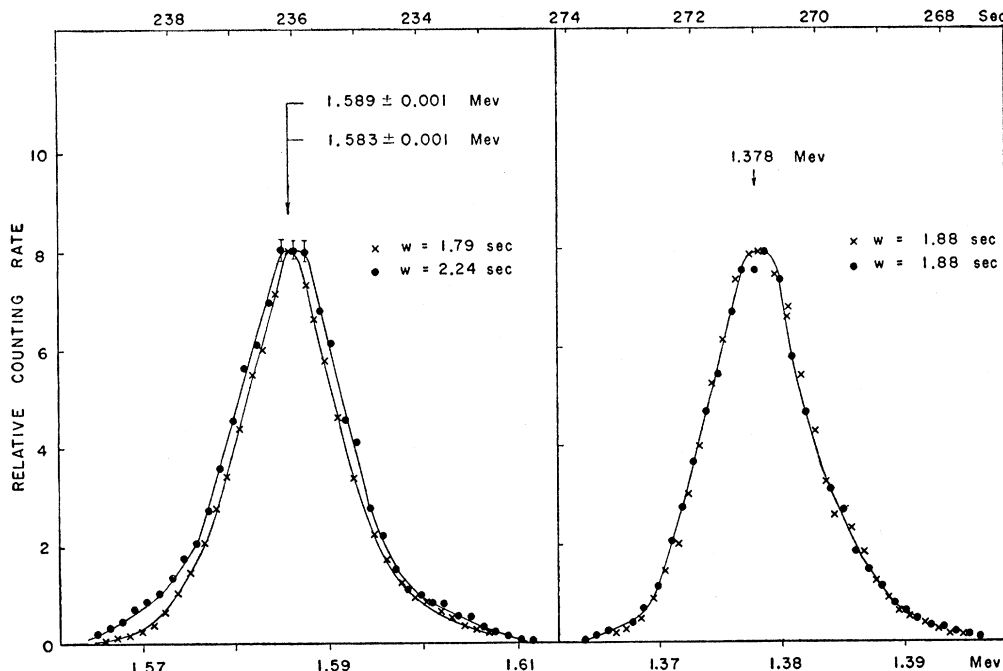


FIG. 3. Measurements of the line shape of the 1.586- and 1.378-Mev  $\gamma$  rays plotted on a linear angle scale, in seconds of arc, and as a function of energy in Mev. The  $\gamma$  rays were measured by Laue diffraction from the (211) planes of two calcite crystals. The measurements were made with the crystals in the antiparallel arrangement (solid circle  $\bullet$ ), which gives maximum energy dispersion, and again with the parallel arrangement (points  $\times$ ) which gives zero energy dispersion. The observed increase in width ( $W$ ) of the antiparallel line is attributed to two  $\gamma$  rays of 1.583 and 1.589 Mev of about equal intensity. For comparison, the 1.378-Mev  $\gamma$  ray was measured and found to have the same shape in the parallel and antiparallel positions.

<sup>20</sup> Bretscher, Alderman, Elwyn, and Shull, Phys. Rev. **96**, 103 (1954).

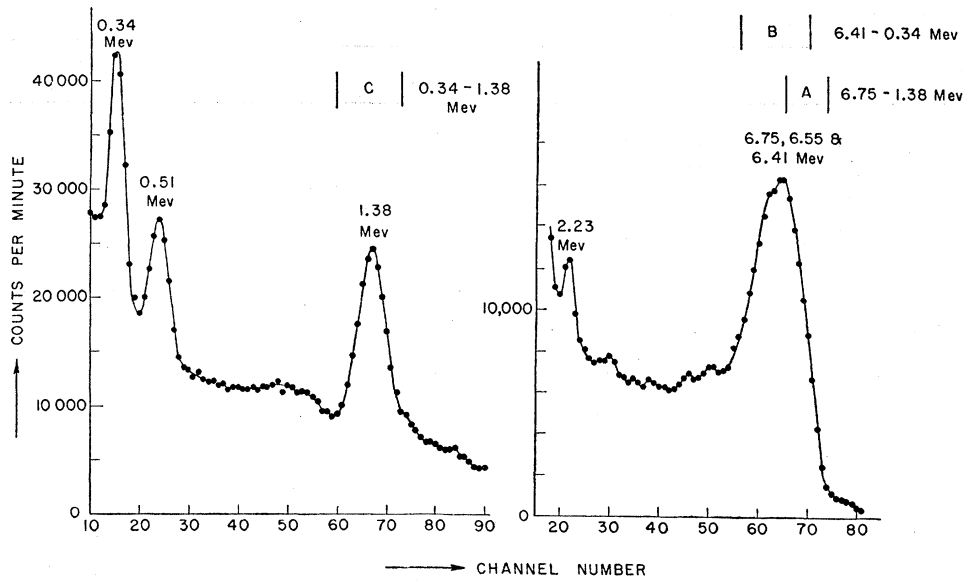


FIG. 4. Typical spectrum observed from a titanium target with one of the scintillation spectrometers used in the angular correlation experiments. The line at 2.23 Mev is from neutron capture in the hydrogen contained in the Lucite target holder. The line at 0.51 Mev is due to annihilation of positrons formed by pair production in materials close to the detector. *A*, *B*, and *C* show the position of the window of the differential discriminator for the coincidence measurements indicated.

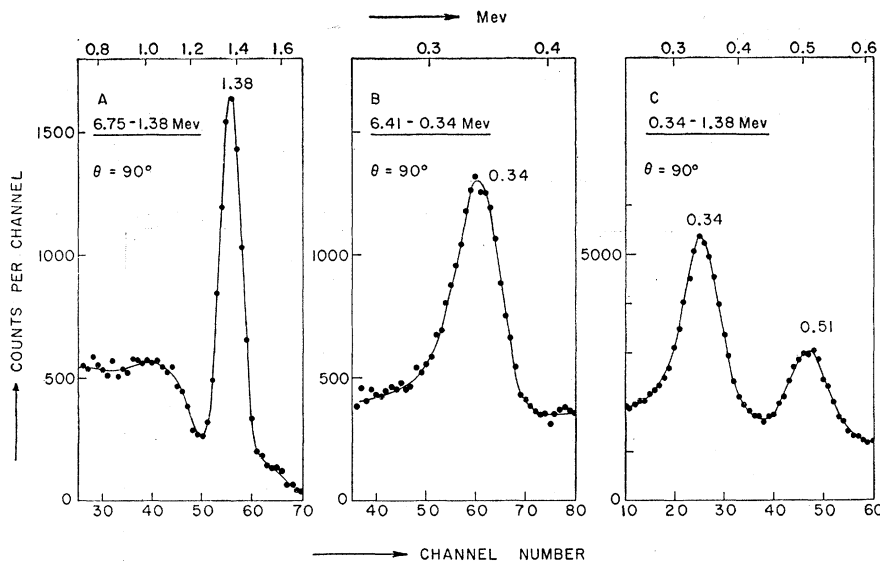


FIG. 5. Typical coincidence spectra obtained with differential discriminator settings as shown in Fig. 4. The spectra shown were obtained with an angle of  $90^\circ$  between the two detectors. The strong 0.51-Mev line is due to annihilation radiation produced by high-energy  $\gamma$  rays which are in coincidence with the 1.38-Mev  $\gamma$  rays.

angular correlation measurements were made in order to confirm these spin assignments. The positions *A*, *B*, and *C* of the fixed differential discriminator for these measurements are shown in Fig. 4, which is a typical spectrum from one of the scintillation detectors. Typical coincidence spectra for these three positions of the differential discriminator are shown in Fig. 5. Position *A* was used to observe the correlation between the 6.75- and 1.38-Mev  $\gamma$  rays.<sup>21</sup> Position *B* was used for the 6.41-0.34-Mev correlation. The 6.75-Mev  $\gamma$  ray is not in coincidence with the 0.34-Mev  $\gamma$  ray and hence there is no complication due to its inclusion in the

<sup>21</sup> There was also some contribution from the 6.41 with 1.38-Mev cascade. However, since the spin of the 1.719-Mev level is ultimately shown to be  $\frac{1}{2}$  the contribution from the 6.41-1.38-Mev cascade is isotropic and does not greatly distort the 6.75-1.38-Mev correlation.

differential discriminator. Position *C* was used for the measurement of the correlation between the 1.38- and 0.34-Mev  $\gamma$  rays.<sup>22</sup> In each case the area under the peak in the coincidence spectrum corresponding to the  $\gamma$  ray being studied was corrected for contributions from higher energy  $\gamma$  rays and was plotted as a function of the angle between the counters. Figures 6(a), 6(b), and 6(c) are the observed correlations for the 6.75-1.38, 6.41-0.34, and 1.38-0.34-Mev cascade transitions, respectively. The observed correlations were fitted by least squares to a function of the form  $W(\theta) = a_0 + a_2 P_2$

<sup>22</sup> There was a small contribution to the observed correlation from pulses from the 6.41-Mev  $\gamma$  ray and other  $\gamma$  rays which fall within the setting *C*. The amount of this contribution was estimated by moving the differential discriminator *C* to just above the 1.38-Mev  $\gamma$  ray. The observed correlation was corrected for this contribution.

( $\cos\theta$ ) where  $P_2(\cos\theta)$  is the Legendre polynomial of the second degree. The fitted functions are given by the full lines in Fig. 6. The expressions at the bottom right of Fig. 6 are the fitted correlations after corrections for the finite size of the target and counters have been applied. These corrections were evaluated using the formulas of Feingold and Frankel<sup>23</sup> and are approximately 18% of the value of  $a_2/a_0$ .

#### IV. INTERPRETATION OF RESULTS

##### IVA. Interpretation of Energy and Intensity Measurements

Neutron capture in natural titanium leads to the formation of the product nuclei  $Ti^{47}$ ,  $Ti^{48}$ ,  $Ti^{49}$ ,  $Ti^{50}$ , and  $Ti^{51}$ . The neutron binding energy of these nuclei and the contribution of the corresponding target nuclei to the capture cross section are given in Table III.

If the binding energies of the product nuclei are multiplied by the fractional contribution of the target nucleus to the total capture cross section<sup>24</sup> an average binding energy of 8.26 Mev is obtained. This figure can be compared with the sum of the products of the resolved  $\gamma$ -ray energies times their intensities in  $\gamma$  rays per capture. This sum is 7.66 Mev which indicates that 93% of the total decay radiation has been resolved.

It is clear from Table III that  $\gamma$  rays with intensities significantly greater than 2.2% per capture in natural titanium must be emitted in the decay of  $Ti^{49}$  and that the most energetic  $\gamma$  rays observed ( $>9$  Mev, Table I) must be emitted in the decay of  $Ti^{48}$  and  $Ti^{50}$ .

Consider first, the decay schemes of  $Ti^{47}$ ,  $Ti^{48}$ , and  $Ti^{50}$ , (Fig. 7).<sup>25</sup> For each of these three nuclei the ground

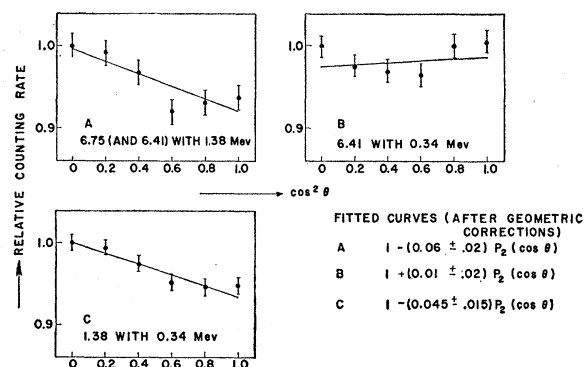


FIG. 6. Observed angular correlations for the 6.75-1.38, 6.41-0.34 and 1.38-0.34-Mev cascades in  $Ti^{49}$ . The values in the bottom right are the correlation functions determined by least squares fitting to the experimental points after corrections have been applied for the finite size of the target and detector.

<sup>23</sup> A. M. Feingold and S. Frankel, Phys. Rev. **97**, 1025 (1955).

<sup>24</sup> Way, King, McGinnis, and van Lieshout, U. S. Atomic Energy Commission Report TID-5300, September, 1955 (unpublished). See also McGinnis, Andersson, Fuller, Mariou, Way, and Yamada, *Nuclear Data Cards* (National Research Council, Washington, D. C., 1958).

<sup>25</sup> The low-binding energy of  $Ti^{51}$ , together with the low cross section for its production, make it difficult to identify  $\gamma$  rays emitted in the  $Ti^{50}(n,\gamma)Ti^{51}$  reaction.

TABLE III. Contribution of target nuclei to thermal capture cross section and neutron binding energies of product nuclei.

Product nucleus	Contribution of target nucleus to cross section <sup>a</sup> (percent)	Neutron binding energy <sup>b</sup> (Mev)
$Ti^{47}$	0.7	$8.885 \pm 0.004$
$Ti^{48}$	2.2	$11.622 \pm 0.004$
$Ti^{49}$	95	$8.145 \pm 0.003$
$Ti^{50}$	1.7	$10.938 \pm 0.003$
$Ti^{51}$	0.3	$6.36 \pm 0.03$

<sup>a</sup> See for example reference 24.

<sup>b</sup> See reference 27.

state  $\gamma$  ray is of too low intensity to be observed. Hence the identification of  $\gamma$  rays emitted in transitions between excited states depends upon a comparison of the energies of the observed  $\gamma$  rays with those predicted by combining the binding energies in Table III with known level energies. In Fig. 7, the energies obtained from other work are shown on the right of the levels. In general, the data are taken from the compilation of Way *et al.*<sup>24</sup>

The 10.621-Mev  $\gamma$  ray can be fitted as a primary transition to the  $0.986 \pm 0.003$ -Mev<sup>26</sup> level in  $Ti^{48}$  since the sum of these energies gives  $11.607 \pm 0.015$  Mev in reasonable agreement with the value  $11.622 \pm 0.004$  Mev obtained from the mass measurements.<sup>27</sup>

The most probable assignment for the 9.376-Mev  $\gamma$  ray is to the primary transition in  $Ti^{50}$  from the capturing state to the level found by Pieper<sup>28</sup> at  $1.58 \pm 0.06$  Mev. A  $\gamma$  ray at  $1.595 \pm 0.014$  Mev observed in the  $Ti^{50}(n,n')Ti^{50}$  reaction by Sinclair<sup>29</sup> is almost certainly emitted in the decay of this level. Assuming this more accurate value for the level energy, we obtain  $10.971 \pm 0.020$  Mev for the neutron binding energy of  $Ti^{50}$ , a value which is some 33 keV higher than the value derived from the mass data, *viz.*,  $10.938 \pm 0.003$  Mev.<sup>27</sup>

The  $\gamma$  ray at 9.189 Mev must be emitted in the decay of either  $Ti^{48}$  or  $Ti^{50}$ . Sinclair<sup>29</sup> has observed  $\gamma$  rays at  $0.998 \pm 0.010$ ,  $1.329 \pm 0.010$ , and  $1.449 \pm 0.018$  Mev following the  $Ti^{48}(n,n')Ti^{48}$  reaction, and has interpreted the third as a transition to the first excited state from a level presumed to lie at 2.447 Mev. Using the more accurate value,  $0.986 \pm 0.003$  Mev<sup>26</sup> for the energy of the first excited state the energy of the level emitting the 1.449-Mev  $\gamma$  ray becomes  $2.435 \pm 0.018$  Mev, in excellent agreement with the energy required to satisfy the 9.189-Mev transition.<sup>30</sup> Since no argument is known for a level at 1.749 Mev in  $Ti^{50}$ , the 9.189-Mev  $\gamma$  ray is assigned to  $Ti^{48}$  as shown in Fig. 7. We also note that the 0.984 and 1.438-Mev  $\gamma$  rays fit very well as the

<sup>26</sup> Van Nooijen, Konijn, Heyligers, Van der Brugge, and Wapstra, *Physica* **23**, 753 (1957).

<sup>27</sup> C. F. Giese and J. L. Benson, Phys. Rev. **110**, 712 (1958).

<sup>28</sup> G. F. Pieper, Phys. Rev. **88**, 1299 (1952).

<sup>29</sup> R. M. Sinclair, Phys. Rev. **107**, 1306 (1957).

<sup>30</sup> Since the capturing state in  $Ti^{48}$  is 2- or 3- a relatively strong primary transition to the 2.435-Mev level is consistent with the 2+ assignment suggested for this level by Sinclair.<sup>29</sup>

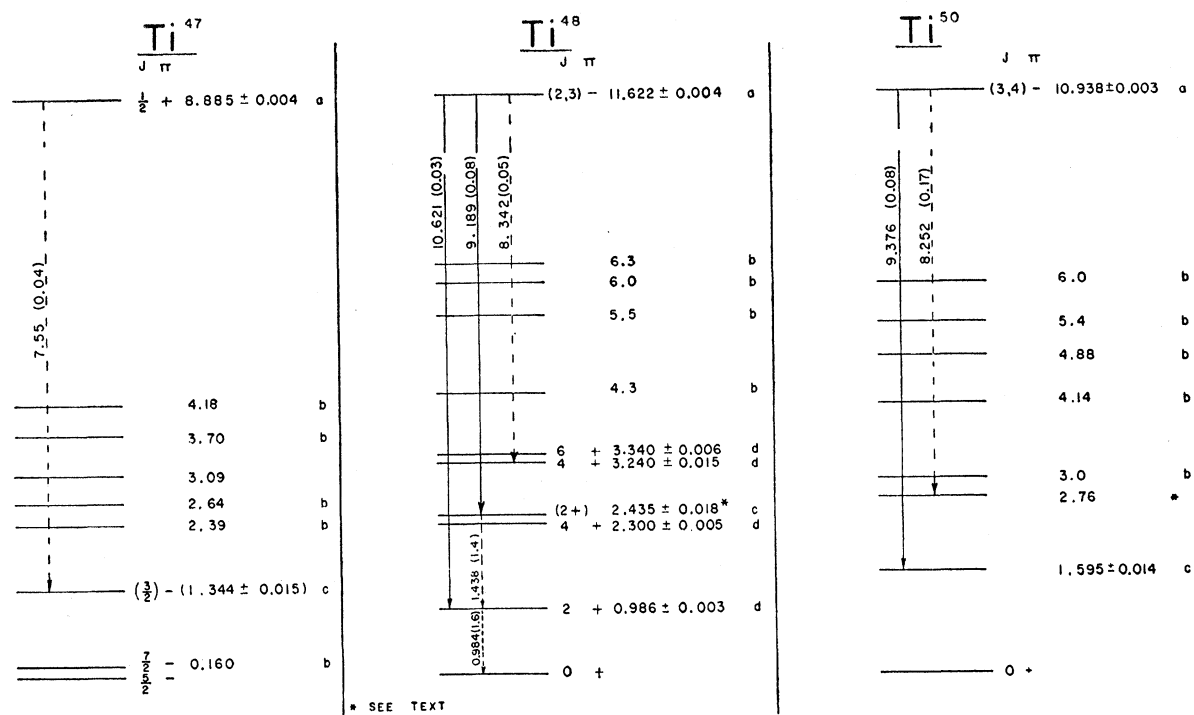


FIG. 7. Decay schemes for  $Ti^{47}$ ,  $Ti^{48}$ , and  $Ti^{50}$ . The level energies are values measured by other workers (references to the literature are given below). The energies and intensities of the  $\gamma$  rays are given on the lines indicating their positions in the decay scheme. Energies are in Mev and the intensities, shown in brackets, are in  $\gamma$  rays per 100 captures in natural titanium.  $J$  and  $\pi$  represent the spins and parities of the levels. The broken arrows indicate assignments of doubtful validity. a, see reference 27; b, see reference 24; c, see reference 29; d, see reference 26.

radiations emitted in the decay of the 0.986- and 2.435-Mev levels. However, such assignments cannot be made with certainty since other locations for these  $\gamma$  rays are possible in the various decay schemes of the titanium isotopes.

The  $\gamma$  ray at 8.342 Mev may be emitted in the transition from the capturing state to the level at  $3.240 \pm 0.015$  Mev<sup>26</sup> in  $Ti^{48}$ . However, the computed level energy,  $3.280 \pm 0.012$  Mev for this transition is in rather poor agreement with the directly measured value and the possibility that this  $\gamma$  ray is emitted in a transition to a previously unobserved level in  $Ti^{47}$  or  $Ti^{50}$  cannot be ruled out.

Although the  $\gamma$  ray at  $8.252 \pm 0.010$  Mev could be interpreted as a primary transition to the level at 3.340 Mev in  $Ti^{48}$  the high spin of this level<sup>26</sup> would appear to rule out such an assignment. A more likely explanation for this  $\gamma$  ray is that it is emitted in a primary transition in  $Ti^{50}$  to a level at approximately 2.76 Mev for which evidence was found in the decay of  $Sc^{50}$  by Morinaga and Bleuler.<sup>31</sup>

Various weak  $\gamma$  rays in the energy range between 7.996 and 6.947 Mev can be assigned to transitions involving known levels in  $Ti^{47}$ ,  $Ti^{48}$ , and  $Ti^{50}$ . For

example, assuming the energy of the second excited state in  $Ti^{47}$  is  $1.344 \pm 0.015$  Mev as suggested by the measurements of Sinclair,<sup>29</sup> the  $7.55 \pm 0.02$ -Mev  $\gamma$  ray may be the expected  $E1$  primary transition to this level. However, for many of the other levels shown in Fig. 7, the errors associated with the level energies are large, and in view of the large number of  $\gamma$  rays, little confidence can be placed in such assignments.

Figure 8, shows the decay scheme for  $Ti^{49}$ . The binding energy obtained by adding the energies of cascading  $\gamma$  rays is  $8.132 \pm 0.006$  Mev in only fair agreement with the value obtained from mass measurements,<sup>27</sup> viz.,  $8.145 \pm 0.003$  Mev. The decay scheme shown differs only in detail from those given by Motz,<sup>2</sup> Adyasevich *et al.*,<sup>3</sup> and Segel.<sup>7</sup> For most  $\gamma$  rays the more accurate measurements reported here, especially at low energies, confirm the earlier assignments by these authors. The doublet at 1.586 Mev is shown as a cascade from a level at 3.172 Mev through a level at 1.583 Mev. The former corresponds to a level at  $3.11 \pm 0.05$  Mev found by  $(d,p)$  measurements.<sup>28</sup> If the  $\gamma$  ray at 4.957 Mev is assumed to be a primary transition to this level its excitation energy is  $3.175 \pm 0.005$  Mev. This is in good agreement with  $3.172 \pm 0.002$  Mev which is the sum of the  $\gamma$ -ray energies assumed to cascade from the level. Previous  $(d,p)$  work has given no indication of a level near 1.586 Mev but the strength

<sup>31</sup> H. Morinaga and E. Bleuler, Phys. Rev. **100**, 1236A (1955). See also compilation by L. J. Lidofsky, Revs. Modern Phys. **29**, 773 (1957).



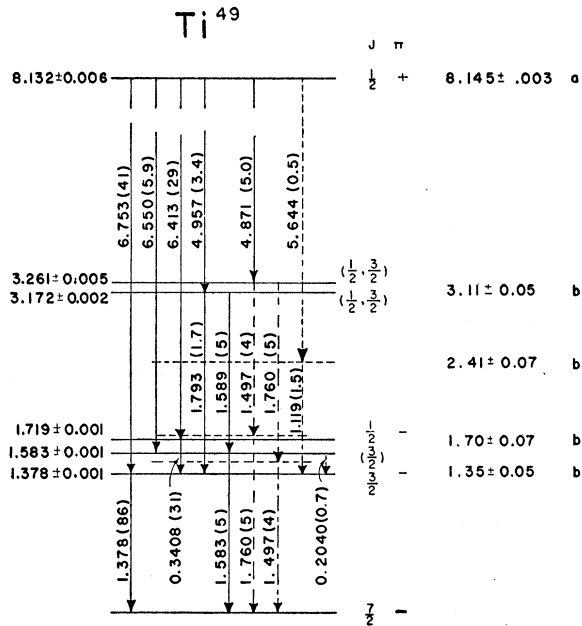


FIG. 8. Decay scheme for  $Ti^{49}$ . The energies to the right of the levels are values measured by other workers (references to the literature are given below). The energies on the left of the levels were deduced from the  $\gamma$ -ray measurements reported here. The energies and intensities are given on the lines indicating their positions in the decay scheme. Energies are in Mev and the intensities, shown in brackets, are in  $\gamma$  rays per 100 captures in  $Ti^{49}$ .  $J$  and  $\pi$  represent the spins and parities of the levels. a, see reference 27; b, see reference 28.

from the 3.261-Mev level to the ground state. The order of the  $\gamma$  rays in the cascade and hence the position of the intermediate state was not determined.

A plausible value for the spin of the 1.583-Mev level can be deduced from the details of the decay scheme. An upper limit to the intensity of a cascade  $\gamma$  ray between the 1.583- and 1.378-Mev levels is 1% per capture. This is definitely less than the full intensity with which the 1.583-Mev level is fed (the primary transition to the level is 6%). If the 1.583-Mev level is assumed to have a spin of  $\frac{1}{2}$ , it would be expected that the transition to the  $\frac{3}{2}$ - level at 1.378 Mev would be  $\sim 10^6$  times as strong as the transition to the  $\frac{1}{2}$ - ground state. The weakness of the transition between the 1.583- and 1.378-Mev levels therefore makes it seem improbable that the former level has a spin of  $\frac{1}{2}$ . On the other hand, the strength of the primary transition to the 1.583-Mev level makes a spin assignment of  $\frac{3}{2}$  improbable. (Using the Weisskopf formula<sup>32</sup> and the observed intensity of the 6.753 and 6.413 Mev  $E1$  transitions, the expected intensity for an  $E2$  transition to the level at 1.583 Mev is  $\sim 0.02\%$  and the observed intensity is  $\sim 6\%$ ). The most probable spin of the 1.583-Mev level is therefore concluded<sup>33</sup> to be  $\frac{3}{2}$ .

The intensities of the primary transitions to the levels at 3.172 and 3.261 Mev indicate that probably each level has a spin of either  $\frac{1}{2}$  or  $\frac{3}{2}$ .

IVB. Interpretation of Angular Correlation Measurements

of the 6.550-Mev  $\gamma$  ray strongly suggests that it is a primary transition to a level at  $1.582 \pm 0.005$  Mev. This value is in good agreement with the energy of the  $\gamma$  ray assumed to depopulate it, viz.,  $1.583 \pm 0.001$  Mev. The 1.497- and 1.760-Mev  $\gamma$  rays are shown as a cascade

Table IV summarizes the data relevant for the analysis of the three correlation measurements. The procedure in the analysis was to use the  $(d,p)$  stripping results of Bretscher *et al.*<sup>20</sup> to limit the considerations of the spin of the 1.378- and 1.719-Mev levels to  $\frac{1}{2}$  or  $\frac{3}{2}$

TABLE IV. Summary of data relevant for the analysis of the  $(\gamma-\gamma)$  angular correlation measurements of  $Ti^{49}$ . Columns 1 and 2 contain the energies (in Mev) of the  $\gamma$  rays in the correlation measurement; columns 3, 4, and 5, the assumed spins and particles of the initial, intermediate and final states of the cascade respectively; columns 6 and 7, the assumed form of radiation for the first and second  $\gamma$  rays, respectively; and columns 8 and 9, the theoretical and experimental values of  $a_2/a_0$ .

	$E_{\gamma 1}$	$E_{\gamma 2}$	$J_i$	$J_{int}$	$J_f$	$\gamma_1$	$\gamma_2$	$a_2/a_0$ Theory <sup>a</sup>	$a_2/a_0$ Expt.
A	6.75	1.38	$\frac{1}{2}+$	$\left\{ \begin{array}{l} \frac{1}{2}- \\ \frac{3}{2}- \end{array} \right.$	$\frac{3}{2}-$	$E1$	$E2$	$\left\{ \begin{array}{l} 0 \\ -0.071 \end{array} \right.$	$-0.06 \pm 0.02$
B	6.41	0.34	$\frac{1}{2}+$	$\left\{ \begin{array}{l} \frac{1}{2}- \\ \frac{3}{2}- \end{array} \right.$	$\frac{3}{2}-$	$E1$	$E2, M1$	$\left\{ \begin{array}{l} 0 \\ \frac{(15)^{\frac{1}{2}}x-1}{5(1+x^2)} \end{array} \right.$	$0.01 \pm 0.02$
C	0.34	1.38	$\left\{ \begin{array}{l} \frac{1}{2}- \\ \frac{3}{2}- \end{array} \right.$	$\frac{3}{2}-$	$\frac{1}{2}-$	$E2, M1$	$E2$	$\left\{ \begin{array}{l} \frac{x^2-2\sqrt{3}x-1}{14(1+x^2)} \\ \frac{2(1-(15)^{\frac{1}{2}}x)}{35(1+x^2)} \end{array} \right.$	$-0.045 \pm 0.015$

<sup>a</sup> The mixture parameter,  $x$ , is the amplitude of the quadrupole radiation divided by the amplitude of the dipole radiation.

<sup>32</sup> J. M. Blatt and V. M. Weisskopf, *Theoretical Nuclear Physics* (John Wiley & Sons, Inc., New York, 1952).

<sup>33</sup> See, however, R. H. Nussbaum, *Revs. Modern Phys.* **28**, 423 (1956).

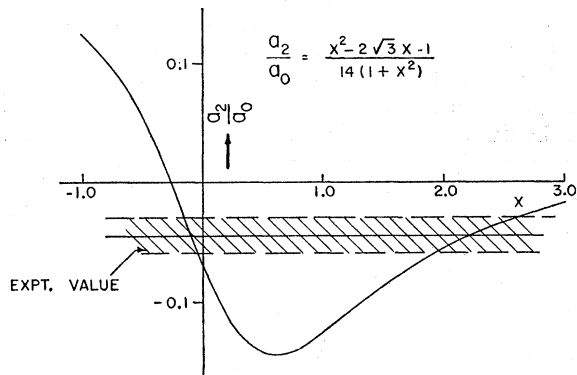


FIG. 9. Theoretical value for  $a_2/a_0$  (coefficient of  $P_2(\cos\theta)$  in correlation function normalized to unity at  $\theta=90^\circ$ ) for the 0.34–1.38-Mev cascade in  $\text{Ti}^{49}$ , plotted against the multipole mixture parameter of the 0.34-Mev  $\gamma$  ray. The shaded region represents the experimental value for  $a_2/a_0$  with its standard deviation errors.

and to fix the parity as negative. The observed correlations were used to choose between these two spin assignments. In Table IV, columns 1 and 2 contain the energies of the  $\gamma$  rays in the correlation measurements; columns 3, 4, and 5, the assumed spins and parities of the initial, intermediate and final states of the cascade respectively; columns 6 and 7, the assumed form of radiation for the first and second  $\gamma$  rays respectively; and columns 8 and 9, the theoretical and experimental values of  $a_2/a_0$ . Correlation *A*, clearly indicates that the 1.378-Mev level is  $\frac{3}{2}^-$ . Correlations *B* and *C* are complicated by the fact that the 0.34-Mev  $\gamma$  ray can be a mixture of *M1* and *E2* radiation. The multipole mixture parameter  $|S_E|/|S_M|$  is defined by Sharp *et al.*<sup>34</sup> and is designated by  $x$ . If the 1.719-Mev level is assumed to be  $\frac{3}{2}^-$  no single value of  $x$  fits both correlations *B* and *C*. The 1.719-Mev level is, therefore, concluded to be  $\frac{1}{2}^-$ . These conclusions confirm the spin assignments of Trumpy<sup>8</sup> for both the 1.378- and 1.719-Mev levels.

Since the 1.719-Mev level is  $\frac{1}{2}^-$  correlation *B* is isotropic but correlation *C* can be used to determine the multipole mixture parameter for the 0.34-Mev  $\gamma$  ray. Figure 9, is a plot of the theoretical value of  $a_2/a_0$  for

<sup>34</sup> Sharp, Kennedy, Sears, and Hoyle, Chalk River Report CRT-556, 1953 (unpublished). We have included the phase corrections of R. Huby, Proc. Phys. Soc. (London) **A67**, 1103 (1954).

the 0.34–1.38-Mev correlation as a function of the multipole mixture parameter for the 0.34-Mev  $\gamma$  ray. The experimental value is shown together with the estimated standard deviation error. The results indicate a value of  $x$  of  $-0.1$  or  $+2.2$ , i.e., an *E2*, *M1* intensity ratio of 0.01 or 5.

## V. DISCUSSION

$\text{Ti}^{49}$  has 22 protons and 27 neutrons. The normally assumed shell model configuration for the nucleus is protons:  $f_{7/2}^2$  and neutrons:  $f_{7/2}^7$ . The neutron configuration may be considered as one hole in the  $f_{7/2}$  shell and the ground-state spin and parity,  $\frac{7}{2}^-$ , are those expected for such a nucleus. The lowest excitations expected are those corresponding to the promotion of the odd uncoupled  $f_{7/2}$  neutron into the next available shells, namely,  $p_{3/2}$ ,  $f_{5/2}$ , and  $p_{1/2}$ . Excitation of the protons is expected to occur at higher energies because of the pairing energy between the two  $f_{7/2}$  protons. The lowest levels of  $\text{Ti}^{49}$  do indeed include levels of  $\frac{3}{2}^-$  and  $\frac{1}{2}^-$  at 1.378 and 1.719 Mev, respectively, but the energy separation between the two levels appears rather smaller than that expected theoretically. Schröder<sup>35</sup> has calculated the energy level sequence for an odd neutron in a potential well, the shape of which was adjusted to obtain the magic numbers. The computed  $p_{3/2}$ ,  $p_{1/2}$  splitting is about 2 Mev for 27 neutrons, while the observed value is 0.34 Mev. On the other hand, the observed splitting for  $\text{Ca}^{41}$  (closed proton and neutron shells plus one  $f_{7/2}$  neutron) is approximately that calculated by Schröder. This may indicate that the model is a reasonable approximation for nuclei near the closed shells at 20 nucleons but is much less valid in the region of  $\text{Ti}^{49}$ . There is evidence<sup>36</sup> that some collective motion may be present in  $\text{Ti}^{48}$ . The small splitting between the assumed  $p_{3/2}$  and  $p_{1/2}$  states in  $\text{Ti}^{49}$  and the possible presence of an *E2*, *M1* mixture for the 0.34-Mev transition<sup>37</sup> between them may be indications that collective effects are present in  $\text{Ti}^{49}$ .

<sup>35</sup> A. Schröder, Nuovo cimento **7**, 461 (1958).

<sup>36</sup> Van Nooijen, Konijn, and Wapstra, Physica **24**, 231 (1958).

<sup>37</sup> The experimental correlation coefficient for the 0.34–1.378-Mev cascade is about 1.8 standard deviations from that expected for pure *M1* radiation. The experiment gives an *E2*/*M1* intensity ratio of 0.01 or 5 which is to be compared with the theoretical value of about  $10^{-8}$  for a single neutron transition between a  $p_{3/2}$  and  $p_{1/2}$  orbit.